

The flow of a layer of non-Newtonian liquid in an open volume is investigated numerically.

Consider the flow of a free layer of non-Newtonian liquid over a plane horizontal surface. Problems of this kind are encountered in the filling of vessels, leakage from reservoirs, the application of polymer coatings, etc. For large liquid volumes, the influence of capillary forces is only large in very thin layers, and is small in ordinary conditions. With slow flow of a highly viscous liquid, the characteristic time of velocity variation is considerably greater than the time of stress relaxation [1], and the elastic properties of the liquid do not appear in its spreading [2]. Therefore, the behavior of a liquid layer is determined only by the character of the stress dependence of its viscosity. In the approximation of a geometrically thin layer ($h_0/L_0 \ll 1$, where h_0 is the layer height, L_0 is the longitudinal scale of flow), the change in form of the layer of non-Newtonian liquid is determined by the equation [2]

$$\frac{\partial h}{\partial t} = \nabla (\rho g f \nabla h), \quad (1)$$

$$f = \int_0^h \Psi [\rho g (h-z) |\nabla h|] (h-z)^2 dz. \quad (2)$$

Equation (1) has a self-similar analytic solution describing axisymmetric spreading of a fixed liquid volume [2]. The comparison in [3] of results of the calculation with experimental data on the spreading of fixed volumes of several polyisobutylene solutions confirms the possibility of using the equations for large times. In the present work, the motion of a non-Newtonian liquid in a volume is numerically investigated. At the walls, the impenetrability condition is imposed, where n is the vector normal

$$\nabla h_r \cdot n = 0. \quad (3)$$

The viscosity function Ψ is determined by a rheological model describing the behavior of a non-Newtonian liquid with shear flow. In the region of relatively low deformation rates, the Ellis model gives good results [4]:

$$\tau = \frac{\eta_0}{1 + \left| \frac{\tau}{\tau_{1/2}} \right|^\alpha} \dot{\gamma}. \quad (4)$$

For $|\tau/\tau_{1/2}| \gg 1$, Eq. (4) reduces to the power law

$$\tau \approx \tau_{1/2} \left(\frac{\eta_0 |\dot{\gamma}|}{\tau_{1/2}} \right)^n \text{sign}(\dot{\gamma}), \quad n = \frac{1}{\alpha + 1}. \quad (4')$$

Equation (1) is solved numerically. Introducing the dimensionless quantities:

$$t = t_0 \bar{t}, \quad X = xL_0, \quad Y = yL_0, \quad h = h_0 \bar{h}, \quad \tau = \tau_* \bar{\tau}, \quad \Psi = \bar{\Psi}/\eta_0.$$

Equations (1) and (2) are rewritten in the form

TABLE 1. Spreading of Liquid Layer (simple alternation of directions)

y	x										
	0,0	0,1	0,2	0,3	0,4	0,5	0,6	0,7	0,8	0,9	1,0
$\bar{t} = 0,01$											
0,0	0,0	0,0	0,0	0,0	0,0	0,0	0,0	0,0	0,0	0,0	0,0
0,1	0,0	0,0	0,0	0,0	0,0	0,0	0,0	0,0	0,0	0,0	0,0
0,2	0,0	0,0	0,004	0,679	0,784	0,801	0,784	0,679	0,004	0,0	0,0
0,3	0,0	0,0	0,702	1,655	1,761	1,781	1,761	1,655	0,702	0,0	0,0
0,4	0,0	0,0	0,790	1,762	1,891	1,917	1,891	1,762	0,790	0,0	0,0
0,5	0,0	0,0	0,804	1,782	1,917	1,945	1,917	1,782	0,804	0,0	0,0
0,6	0,0	0,0	0,790	1,762	1,891	1,917	1,891	1,762	0,790	0,0	0,0
0,7	0,0	0,0	0,702	1,655	1,761	1,781	1,761	1,655	0,702	0,0	0,0
0,8	0,0	0,0	0,004	0,679	0,784	0,801	0,784	0,679	0,004	0,0	0,0
0,9	0,0	0,0	0,0	0,0	0,0	0,0	0,0	0,0	0,0	0,0	0,0
1,0	0,0	0,0	0,0	0,0	0,0	0,0	0,0	0,0	0,0	0,0	0,0

TABLE 2. Spreading of a Layer of Non-Newtonian Liquid (Ellis model, $C = 1, \alpha = 1.5$)

y	x										
	0,0	0,1	0,2	0,3	0,4	0,5	0,6	0,7	0,8	0,9	1,0
$\bar{t} = 0,50; \quad \Delta \bar{t} = 1,06 \cdot 10^{-2}$											
0,0	0,356	0,377	0,431	0,498	0,551	0,572	0,551	0,498	0,431	0,377	0,356
0,1	0,377	0,399	0,456	0,527	0,583	0,605	0,583	0,527	0,456	0,399	0,377
0,2	0,431	0,456	0,522	0,602	0,667	0,692	0,667	0,602	0,522	0,456	0,431
0,3	0,498	0,527	0,602	0,696	0,771	0,799	0,771	0,696	0,602	0,527	0,498
0,4	0,551	0,583	0,667	0,771	0,854	0,885	0,854	0,771	0,667	0,583	0,551
0,5	0,572	0,605	0,692	0,799	0,885	0,918	0,885	0,799	0,692	0,605	0,572
0,6	0,551	0,583	0,667	0,771	0,854	0,885	0,854	0,771	0,667	0,583	0,551
0,7	0,498	0,526	0,602	0,696	0,771	0,799	0,771	0,696	0,602	0,526	0,498
0,8	0,431	0,456	0,522	0,602	0,667	0,692	0,667	0,602	0,522	0,456	0,431
0,9	0,377	0,399	0,456	0,527	0,583	0,605	0,583	0,527	0,456	0,399	0,377
1,0	0,356	0,377	0,431	0,498	0,551	0,572	0,551	0,498	0,431	0,377	0,356

$$\frac{\partial \bar{h}}{\partial \bar{t}} = \frac{\partial}{\partial x} \left(\bar{h}^3 \zeta \frac{\partial \bar{h}}{\partial x} \right) + \frac{\partial}{\partial y} \left(\bar{h}^3 \zeta \frac{\partial \bar{h}}{\partial y} \right), \quad (5)$$

$$\zeta = \int_0^1 (1 - \xi)^2 \bar{\Psi} [C \bar{h} |\nabla \bar{h}| (1 - \xi)] d\xi. \quad (6)$$

$C = \rho g h_0^2 / L_0 \tau_*$, $t_0 = \eta_0 L_0^2 / \rho g h_0^3$, and τ_* is the stress scale. The principal feature of the non-Newtonian liquid is that the function ζ depends on the layer height \bar{h} and the gradient $|\nabla \bar{h}|$. Thus, for a Newtonian liquid $\zeta = 1/3$, while for the Ellis model

$$\zeta = \left[\frac{1}{3} + \frac{1}{\alpha + 3} (C \bar{h} |\nabla \bar{h}|)^\alpha \right], \quad \tau_* = \tau_{1/2}. \quad (7)$$

The method of directional splitting is used to solve Eq. (5) [5]. Two grid functions are introduced: for integer nodes of the grid, $W_{ijk} = \{t_k, x_i, y_j\}$; for semiinteger nodes, $\bar{W}_{ijk} = \{x_{i+1/2}, y_{j+1/2}, t_{k+1/2}\}$. In this case, Eq. (5) is divided in two, each describing spreading along only a single axis (OX or OY)

$$\frac{\bar{h}_{ij}^{k+1} - \bar{h}_{ij}^{k+1/2}}{2\Delta \bar{t}_k} (\Delta x_i + \Delta x_{i-1}) = \frac{\bar{h}_{i+1,j}^{k+1} - \bar{h}_{ij}^{k+1}}{\Delta x_i} E_{i+1,j}^{k+1} - \frac{\bar{h}_{ij}^{k+1} - \bar{h}_{i-1,j}^{k+1}}{\Delta x_{i-1}} E_{i,j}^{k+1}, \quad (8)$$

$$\frac{\bar{h}_{ij}^{k+1/2} - \bar{h}_{ij}^k}{2\Delta \bar{t}_k} (\Delta y_j + \Delta y_{j-1}) = \frac{\bar{h}_{i,j+1}^{k+1/2} - \bar{h}_{ij}^{k+1/2}}{\Delta y_j} E_{i,j+1}^{k+1} - \frac{\bar{h}_{ij}^{k+1/2} - \bar{h}_{i,j-1}^{k+1/2}}{\Delta y_{j-1}} E_{i,j}^{k+1}.$$

It is evident that transition from the k -th to the $(k+1)$ -th time layer occurs using the intermediate time layer $k + 1/2$, i.e., a half time step $\Delta \bar{t}_k / 2$ is used in solving the problem.

The integrointerpolational method of [6], which gives a conservative difference scheme, is used to obtain Eq. (8). The given equations ensure conservation of the quantity

$$H = \frac{1}{2} \sum_{i=1}^{N_1} (\bar{h}_{i1} \Delta x_i \Delta y_1 + \bar{h}_{i, N_2} \Delta x_i \Delta y_{N_2}) + \sum_{i=2}^{N_1-1} \sum_{j=2}^{N_2-1} \bar{h}_{ij} \Delta x_i \Delta y_j + \frac{1}{2} \sum_{j=2}^{N_2-1} (\bar{h}_{1j} \Delta x_1 \Delta y_j + \bar{h}_{N_1, j} \Delta x_{N_1} \Delta y_j),$$

which is an analog of the volume of the spreading liquid layer. The mass-transfer coefficients $E_{i+1, j}^{k+1}$ and $E_{i, j+1}^{k+1}$ are determined from the formulas [6]

$$E_{i+1, j}^{k+1} = \frac{1}{\Delta x_i \int_{x_i}^{x_{i+1}} \frac{dx}{\bar{h}^3 \zeta(\bar{h}, |\nabla \bar{h}|)}} \approx (\bar{h}^3 \zeta)_{i+1/2, j}^{k+1},$$

$$E_{i, j+1}^{k+1} = \frac{1}{\Delta y_j \int_{y_j}^{y_{j+1}} \frac{dy}{\bar{h}^3 \zeta(\bar{h}, |\nabla \bar{h}|)}} \approx (\bar{h}^3 \zeta)_{i, j+1/2}^{k+1}.$$

In calculating ζ at semiinteger nodes, the following expressions are used

$$\bar{h}_{i+1/2, j} = \frac{\bar{h}_{i+1, j} + \bar{h}_{ij}}{2}, \quad \left(\frac{\partial \bar{h}}{\partial x} \right)_{i+1/2, j} = \frac{\bar{h}_{i+1, j} - \bar{h}_{ij}}{\Delta x_i},$$

$$\left(\frac{\partial \bar{h}}{\partial y} \right)_{i+1/2, j} = \frac{\bar{h}_{i+1, j+1} + \bar{h}_{i, j+1} - \bar{h}_{i, j-1} - \bar{h}_{i+1, j-1}}{2(\Delta y_{j+1} - \Delta y_j)},$$

$$\bar{h}_{i, j+1/2} = \frac{\bar{h}_{i, j+1} + \bar{h}_{ij}}{2}, \quad \left(\frac{\partial \bar{h}}{\partial y} \right)_{i, j+1/2} = \frac{\bar{h}_{i, j+1} - \bar{h}_{ij}}{\Delta y_j},$$

$$\left(\frac{\partial \bar{h}}{\partial x} \right)_{i, j+1/2} = \frac{\bar{h}_{i+1, j+1} + \bar{h}_{i+1, j} - \bar{h}_{i-1, j} - \bar{h}_{i-1, j+1}}{2(\Delta x_{i+1} - \Delta x_i)}.$$

The replacement of derivatives by difference ratios in this way results from the need to construct symmetric formulas in terms of the variables x, y . At the boundary of the region, the impenetrability conditions are specified

$$\left(\frac{\partial \bar{h}}{\partial x} \right)_{i+1/2, 1} = \left(\frac{\partial \bar{h}}{\partial x} \right)_{i+1/2, N_2} = 0, \quad \left(\frac{\partial \bar{h}}{\partial y} \right)_{1, j+1/2} = \left(\frac{\partial \bar{h}}{\partial y} \right)_{N_1, j+1/2} = 0.$$

At the corners $(x_1, y_1), (x_1, y_{N_2}), (x_{N_1}, y_1), (x_{N_1}, y_{N_2})$ both the derivatives are set equal to zero.

The system in Eq. (8) is nonlinear with respect to \bar{h}_{ij}^{k+1} . It is solved by an iterative method. The iterative process, which refines the values of the functions $E_{ij}^{k+1}(\bar{h}_{ij}^{k+1}, |\nabla \bar{h}_{ij}^{k+1}|)$ depending on the desired solution, is constructed by the following linearization of Eq. (8),

$$\bar{h}_{ij}^{k+1} \rightarrow \bar{h}_{ij}^{k+1, \alpha}; E_{ij}^{k+1}(\bar{h}^{k+1}, |\nabla \bar{h}^{k+1}|) \rightarrow E_{ij}^{k+1}(\bar{h}^{k+1, \alpha-1}, |\nabla \bar{h}^{k+1, \alpha-1}|),$$

where $\bar{h}_{ij}^{k+1, \alpha}$ is the value of the α -th iteration. The value of the function in the preceding time layer $\bar{h}_{ij}^{k+1, 0} = \bar{h}_{ij}^k$ is taken as the initial iteration. The difference scheme is linear relative to $\bar{h}_{ij}^{k+1, \alpha}$. Systematic calculation of the iterations continues until

$$\varepsilon \geq \max_{i, j} |\bar{h}_{ij}^{k+1, \alpha} - \bar{h}_{ij}^{k+1, \alpha-1}|, \quad (9)$$

where ε is the specified accuracy.

To reduce the time for numerical solution of the problem, automatic correction of the time step in the calculation is performed. This allows the maximum possible step $\Delta \bar{t}_k$ to be determined for the specified accuracy ε . The correction proceeds as follows. If the number of iterations $N_{um} < N_{min}$, the step is increased q times in a numerical progression, where $q = 1.01-1.05$. When $N_{um} > N_{min}$ but $N_{um} < N_{mid}$, the step is increased in an arithmetic pro-

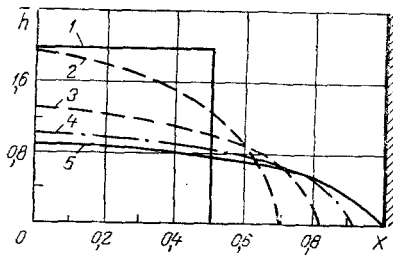


Fig. 1. Variation in layer height along the axis OX over time: 1) $t = 0$; 2) 0.05; 3) 0.20; 4) 0.50; 5) 4.0.

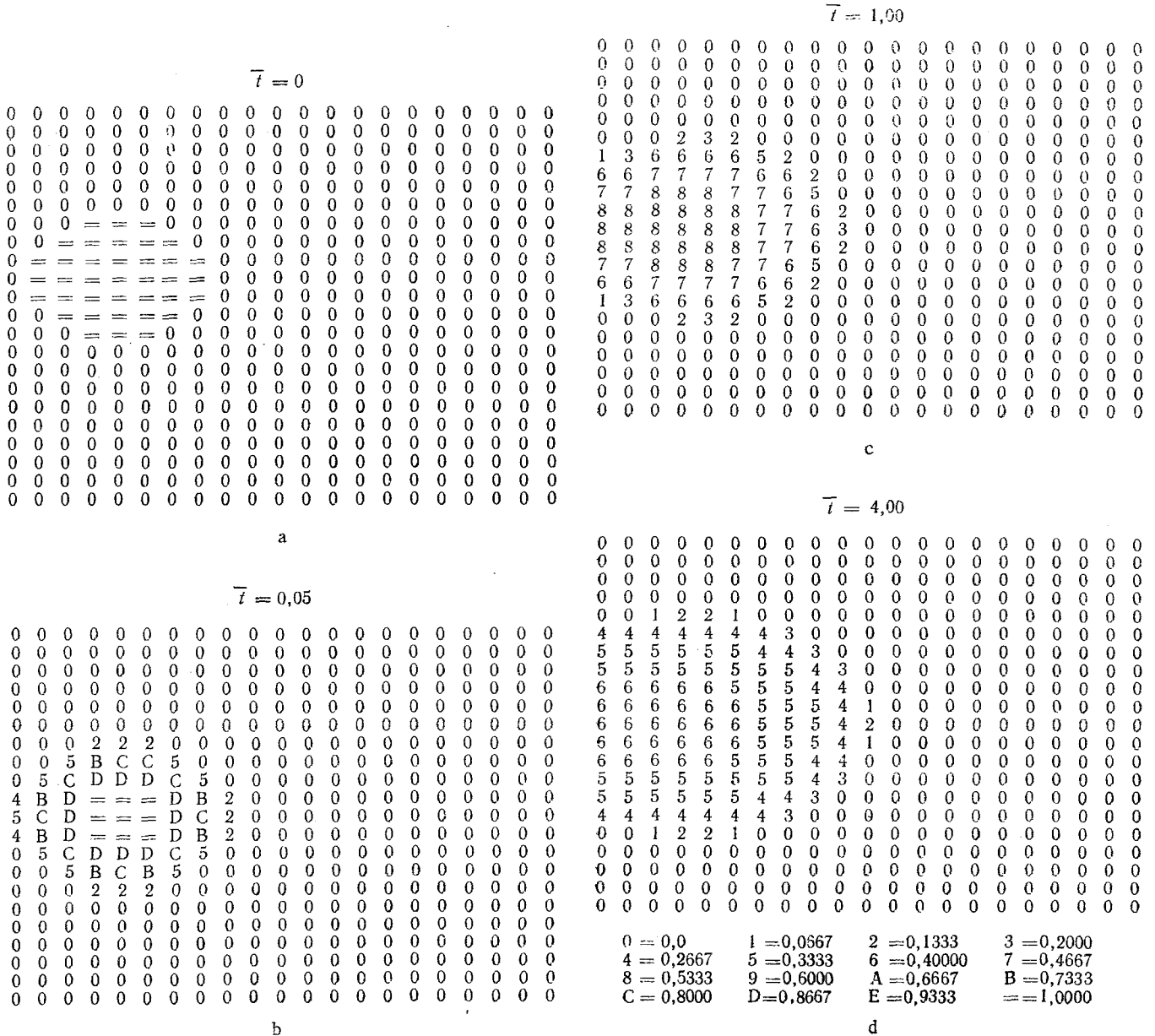


Fig. 2. Spreading of a cylinder of height $\bar{h} = 1.0$ at the wall: $\bar{t} = 0$ (a), 0.05 (b), 1.0 (c), 4.0 (d).

gression: $\Delta \bar{t}_{k+1} = \Delta \bar{t}_k + 0,001 \Delta \bar{t}_1$; otherwise it is unchanged. If the iterative process does not converge for $N_{um} > N_{max}$, the step is halved for the specified accuracy ϵ . The values taken for N_{min} , N_{max} , N_{mid} are 3, 15, 8. The initial step is $\Delta \bar{t}_1 = \Delta x_1^2$ and the maximum time step Δt_m is bounded by the value $\Delta \bar{t}_m \sim \Delta x_1$. The gain in computation time depends strongly on the degree of nonlinearity of the problem being solved, but amounts to a factor of 2-3 on average in comparison with the use of a constant step. With simple alternation of direction, the second relation in Eq. (8) is first solved. Then, using $\bar{h}^{k+1/2, \alpha}_{ij}$, the first equation is

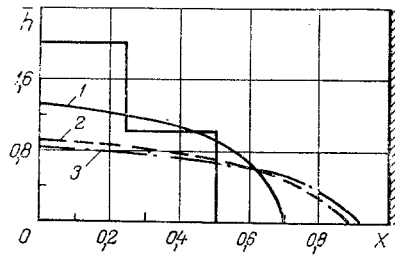


Fig. 3. Influence of C on the spreading of a layer with $\alpha = 1$ for $\bar{t} = 0.01$: 1) $C = 1$; 2) 5; 3) 10.

solved for $\bar{h}^{k+1, \alpha}_{ij}$. Next, the solution obtained is used as the iteration for the calculation of the new values of $E^{k+1, \alpha}_{ij}$, and the cycle is repeated. This scheme was used in [7] to find the concentration distribution of the elements in diffusional processes, where they gave good results in view of the weak nonlinearity of the problem (the diffusion coefficients depend only on the concentration).

As a result of a series of model calculations, good conservation of the overall volume of the liquid layer is established (the relative error is of the order of 0.1%). Simultaneously, it is found that, with increase in computation time, the asymmetry in the layer-height distribution increases. Thus, in the spreading of a liquid parallelepiped at the center of a square area of dimensions 1×1 , the height distribution is asymmetric. The asymmetry increases over time, reaching a maximum, and then decreases on account of smoothing of the height difference. Table 1 gives the layer-height distribution for a Newtonian liquid with a square initial cross section. The computational time step is $\Delta \bar{t} \sim 10^{-3}$. It is evident that, for the given initially symmetric problem, the height distribution is asymmetric even at time $\bar{t} = 0.01$. Thus, the use of the splitting method does not allow sufficiently large steps to be used ($\Delta \bar{t} \sim 0.01$). This constraint was also noted in [8].

To eliminate this deficiency of the splitting method, systematic variation in the alternation of directions is applied. The solution obtained in the preceding time layer is taken as the initial, zero iteration. Then the height distribution in the next half time step is considered. It is the initial distribution for calculating the height in the $(k + 1)$ -th layer. The calculation of the $(k + 1/2)$ -th layer proceeds along the axis OX and that of the $(k + 1)$ -th layer along the axis OY . The solution obtained is the first approximation for the subsequent iterative process. However, in the next semiinteger time layer, the calculation is not along OX but along OY . The calculation of the $(k + 1)$ -th layer changes correspondingly; it proceeds along OX . If the condition in Eq. (9) is not satisfied, the solution obtained is used to calculate the coefficients $E^{k+1, \alpha}_{ij}$ and the iterative process is repeated. The iteration is concluded after Eq. (9) is satisfied. In the course of all the calculations, regardless of the satisfaction of Eq. (9), systematic alternation of the directions for the integer and semiinteger time layers is undertaken. The results of calculations by the given scheme show that the form of the layer surface is practically symmetric. The relative error is no greater than 0.1% for any time step $\Delta \bar{t}_k$.

The variation of the layer height of the non-Newtonian liquid along the axis OX passing through the midpoint of the area is shown in Fig. 1. The dependence of the tangential stress on the velocity is described by Eq. (4) with $C = 1$ and $\alpha = 1.0$. It is evident that the velocity of spreading reduces over time because of the decrease in the difference along the layer. Table 2 gives height values at time $\bar{t} = 0.50$ and the corresponding integration step. The solution employs systematic alternation of the direction. It is evident that the height distribution is symmetric. A liquid column of square form is gradually converted to a circle. Filling of the corners of the volume by liquid occurs in the final stages. The spreading of a cylinder under the action of its weight is shown in Fig. 2. The closeness of the volume walls significantly influences the change in form of the layer (Fig. 2). For $\bar{t} \geq 1$, motion occurs basically from the wall. Up to time $\bar{t} = 4.00$, it resembles the flow in the filling of a volume through its side wall, part of which is removed at $\bar{t} = 0$.

The degree of non-Newtonian behavior of the liquid (α and the dimensionless complex C) exerts a strong influence on the form of the spreading layer and its velocity of motion over the surface. With identical values of α , increase in C is associated with decrease in the stress τ_* , with constant scales h_0, L_0, n_0 . The influence of C on the spreading of a liquid layer consisting of two cylinders is shown in Fig. 3. It is evident that the spreading rate increases with increase in C .

Variation in α at constant C leads to change in form of the flow front of the layer: the larger α , the steeper the front.

The results of the calculations show that the use of the splitting method with systematic variation in the alternation of the directions allows efficient difference schemes to be constructed for the solution of two-dimensional problems of the spreading of non-Newtonian liquids and allows sufficiently large time steps to be used.

NOTATION

h , layer height, m; t , time, sec; ρ , density, kg/m^3 ; g , acceleration due to gravity, m/sec^2 ; τ , tangential stress, N/m^2 ; η , viscosity, $\text{Pa}\cdot\text{sec}$; γ , shear velocity, sec^{-1} ; h_0, L_0, t_0 , height, length, and time scales; η_0 , greatest Newtonian viscosity; $\tau_{1/2}$, stress at which viscosity is halved; τ_* , stress scale; n, α , indices of non-Newtonian behavior of liquid; ψ , viscosity function.

LITERATURE CITED

1. G. Astarita and G. Marrucci, Principles of Non-Newtonian Fluid Mechanics, McGraw-Hill, (1974).
2. B. M. Khusid, "Spreading of a non-Newtonian liquid over a horizontal plane with intense heat and mass transfer at the layer surface," *Inzh.-Fiz. Zh.*, 45, No. 1, 51-60 (1983).
3. A. A. Dunets, B. M. Khusid, O. I. Mikulin, and L. P. Pripasaeva, "Spreading of non-Newtonian liquid over a horizontal surface under the action of its weight," in: Non-steady Processes of Rheodynamics and Heat and Mass Transfer [in Russian], ITMO im. A. V. Lykova Akad. Nauk BSSR, Minsk (1983), pp. 88-92.
4. V. P. Shul'man, S. M. Aleinikov, B. M. Khusid, and É. É. Yakobson, Rheological Equations of State of Viscous Polymer Media (Analysis of the State of the Problem). Preprint No. 13 [in Russian], A. V. Lykov Institute of Heat and Mass Transfer, Academy of Sciences of the Belorussian SSR, Minsk (1981).
5. N. N. Yanenko and V. M. Kovenya, Splitting Method in Gasdynamics Problems [in Russian], Nauka, Siberian Branch, Novosibirsk (1981).
6. A. A. Samarskii, Theory of Difference Schemes [in Russian], Nauka, Moscow (1983).
7. L. G. Voroshin and B. M. Khusid, Diffusional Mass Transfer in Multicomponent Systems [in Russian], Nauka i Tekhnika, Minsk (1979).
8. A. D. Gadzhiev and V. N. Pisarev, "'Romb' implicit finite-difference method for numerical solution of gasdynamic equations with heat conduction," *Zh. Vychisl. Mat. Mat. Fiz.*, 19, No. 15, 1288-1303 (1979).